

AD-722 238

800-786

USADAC TECHNICAL LIBRARY



5 0712 01018685 5

2 Tech Lib Fil

86

COPY NO. _____

TECHNICAL REPORT 4152

FAILURE OF ADHESIVE BONDS
AT
CONSTANT STRAIN RATES



BY

ELISE MCABEE
MICHAEL J. BODNAR
WILLIAM C. TANNER
DAVID W. LEVI

MARCH 1971

APPROVED FOR PUBLIC RELEASE; DISTRIBUTION UNLIMITED

PICATINNY ARSENAL
DOVER, NEW JERSEY

25 APR 1971

The findings in this report are not to be construed
as an official Department of the Army position.

DISPOSITION

Destroy this report when no longer needed. Do not
return to the originator.

Technical Report 4152

FAILURE OF ADHESIVE BONDS AT CONSTANT STRAIN RATES

by

Elise McAbee
Michael J. Bodnar
William C. Tanner
David W. Levi

March 1971

Approved for public release; distribution is unlimited.

AMCMS Code 4010.28.9.02003

Materials Engineering Laboratory
Feltman Research Laboratories
Picatinny Arsenal
Dover, N. J.

ACKNOWLEDGMENTS

The constant stress data was provided by Mr. R. F. Wegman. Thanks are also due Mrs. Dorothy Teetsel for assistance with the manuscript.

TABLE OF CONTENTS

	Page No.
Object	1
Summary	1
Introduction	1
Results and Discussion	1
Experimental Procedure	4
Materials	4
Preparation of Adherends	5
Preparation of Lap Shear Specimens	5
Specimen Testing	5
References	6
Distribution List	27
Tables	
1 Failure data for AF126 adhesive with 1/8 inch thick aluminum adherends at constant strain rate	7
2 Failure data for AF126 adhesive with 1/16 inch aluminum adherends at constant strain rate	8
3 Deformation from C and t_f values	9
4 Deformation from $\log C$ versus $\log (1/t_f)$ plots	10
5 β Values from slopes of the various plots	11

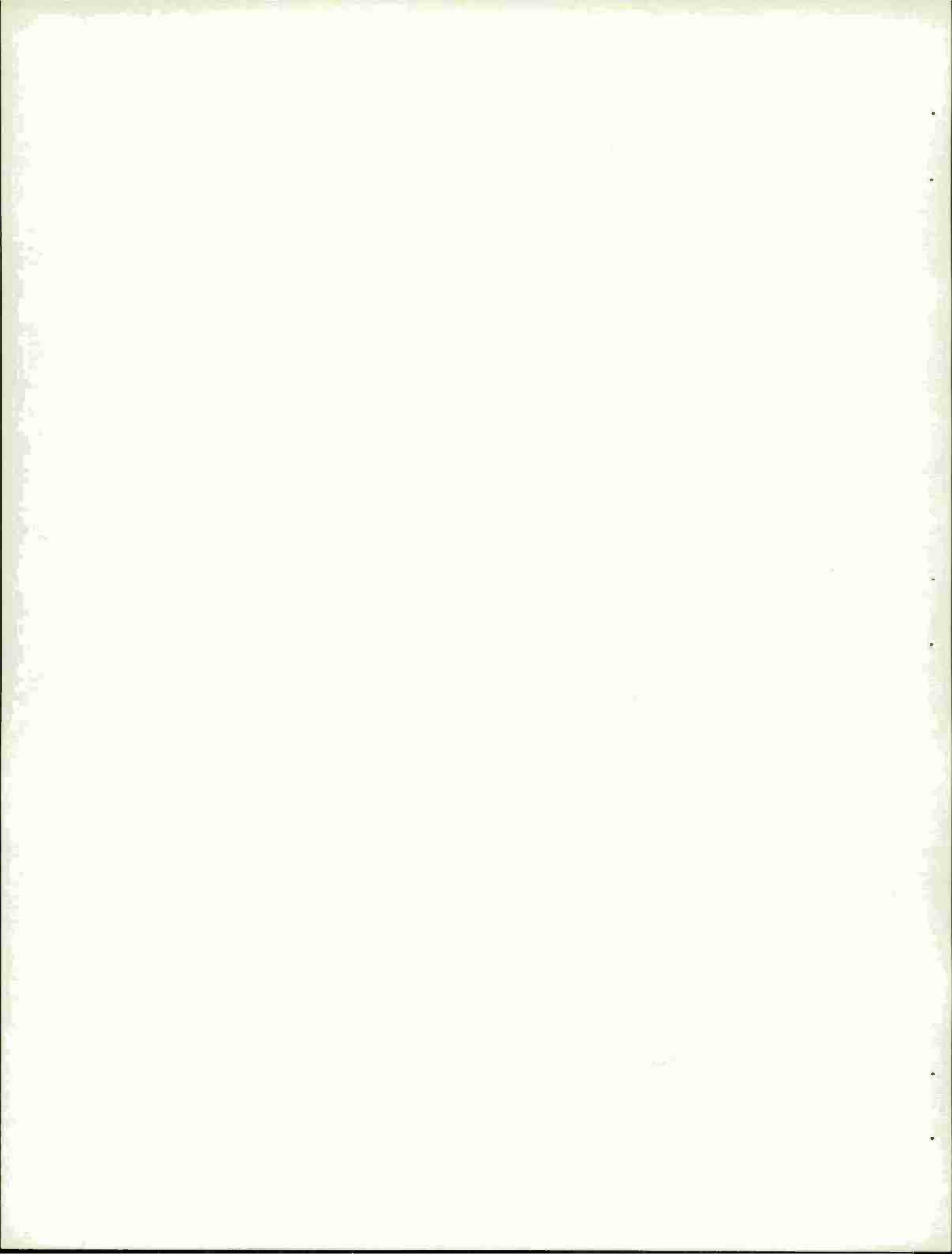
6	Variation of average δ values with temperature	12
7	δ Values derived from constant stress data	13

Figures

1	S versus log C for AF126 adhesive with 1/8" aluminum adherends	14
2	S versus log C for AF126 adhesive with 1/16" aluminum adherends	15
3	S/T versus log C for AF126 adhesive with 1/8" aluminum adherends	16
4	S/T versus log C for AF126 adhesive with 1/16" aluminum adherends	17
5	Log C versus log $(1/t_f)$ for AF126 adhesive with 1/8" aluminum adherends	18
6	Log C versus log $(1/t_f)$ for AF126 adhesive with 1/16" aluminum adherends	19
7	S versus log $(1/t_f)$ for AF126 adhesive with 1/8" aluminum adherends	20
8	S versus log $(1/t_f)$ for AF126 adhesive with 1/16" aluminum adherends	21
9	S/T versus log $(1/t_f)$ for AF126 adhesive with 1/8" aluminum adherends	22
10	S/T versus log $(1/t_f)$ for AF126 adhesive with 1/16" aluminum adherends	23
11	S versus log t_f for AF126 adhesive with 1/16" aluminum adherends. 20% Relative humidity	24

12 S versus $\log t_f$ for AF126 adhesive with 1/16" aluminum adherends. 50% Relative humidity 25

13 S versus $\log t_f$ for AF126 adhesive with 1/16" aluminum adherends. 90-95% Relative humidity 26



OBJECT

The object of this work was to study the shear strength of a structural adhesive used in Army helicopters as a function of strain rate and failure time at several temperatures.

SUMMARY

Shear strengths of adhesive AF126 bonds to two thicknesses of aluminum were measured at constant rate of crosshead separation. Primarily cohesive failure was observed in all cases. By using relations proposed by Cherry and Holmes, the shear strength could be quantitatively related to temperature and strain rate or failure time. Of specific engineering interest would be the possibility of determining the reliability of a bonded joint for specific periods of time as a function of continuously applied stress at a given temperature.

INTRODUCTION

Scientists in the Materials Engineering Laboratory at Picatinny Arsenal have in the past shown some interest in the causes of failure of adhesive bonds under various loading conditions (Refs 1, 2). More recently, some constant strain rate shear strength determinations have been made on an AF126 adhesive used for structural bonding in Army helicopters. This paper shows that the shear strength of such a bond, under conditions where cohesive failure occurs, can be quantitatively related to temperature and strain rate or failure time.

RESULTS AND DISCUSSION

Tables 1 and 2 show the data for the constant strain rate (constant crosshead separation) measurements on 1/8 inch and 1/16 inch aluminum adherends bonded with AF126 adhesive. Three crosshead rates (0.105, 0.8, and 2 in. per min) were used at each of six temperatures (193° , 233° , 273° , 296° , 323° , and 343° K).

Cherry and Holmes (Ref 3) suggested that when a shear stress is applied to a polymer there is an instantaneous elastic deformation resulting from bond angle bending as well as simultaneous plastic deformation, stretching the polymer chains joining adjacent slipped

areas of the polymer until these chains break. When a critical rate of chain scission is exceeded, catastrophic failure occurs. For constant strain rate experiments, they obtained the relation

$$S = (2kT/\beta) \ln C + (2kT/\beta) \ln(hl/\rho \beta RT) + (2RG_e)^{1/2} + 2\varepsilon_0/\beta \quad (1)$$

S is stress at failure, β is volume of elements that respond in failure, C is rate of crosshead separation, l is diameter of "dislocation loop", ρ is density of dislocation lines in unit volume of the medium, $(2RG_e)^{1/2}$ is a critical value of strain at failure, and ε_0 is an activation energy barrier. Since the last three terms on the right-hand side of Equation 1 are constant at a given temperature, this equation requires that a plot of S versus $\log C$ be linear. Figures 1 and 2 show such plots for the data given in Tables 1 and 2.

An alternative form of Equation 1 may be obtained by dividing through by T

$$S/T = (2k/\beta) \ln C + \frac{2k}{\beta} \ln \left(\frac{hl}{\rho \beta RT} \right) + \frac{(2RG_e)^{1/2}}{T} + \frac{2\varepsilon_0}{\beta T} \quad (2)$$

In this case, the S/T vs $\log C$ plots should be linear for each temperature. Figures 3 and 4 show the appropriate straight lines.

Equations 1 and 2 suggest that S or S/T should also be linear with $\log(1/t_f)$. This will be so if the deformation (ε) is constant at a given temperature. (t_f is failure time.)

$$Ct_f = \varepsilon \quad (3)$$

The Ct_f products shown in Table 3 give an indication of the constancy of ε at each temperature. For 1/16 inch aluminum in the three cases where values are not recorded, the machine stalled on release, leading to a hesitation and longer times than would otherwise have been observed. A somewhat more convenient representation can be given by rearranging Equation 3 and taking logarithms.

$$\log C = \log \varepsilon + \log(1/t_f) \quad (4)$$

Equation 4 shows that a plot of $\log C$ versus $\log (1/t_f)$ drawn with a slope = 1 will yield β at $\log (1/t_f) = 0$. Figures 5 and 6 show the straight lines drawn with slope = 1 in each case. Values of $\log \beta$ obtained from these lines are given in Table 4.

It is interesting to note that there appears to be a small but noticeable variation of deformation with temperature for the samples using 1/8 inch aluminum adherends. In the case of 1/16 inch aluminum adherends, the deformation does not appear to vary with temperature, at least beyond the range of experimental error. The deformation (as used in this report and calculated from the observed C and t_f values) is presumably made up of grip slippage, and deformation in the links of the machine, the aluminum metal adherends, and the adhesive. The 1/16 inch aluminum adherends deform visibly under the test conditions while the 1/8 inch aluminum adherends do not. The observed differences are probably due to this difference in the response of the aluminum.

The reasonable constancy of the deformation at a given temperature for each of the crosshead rates makes it possible to replace $\log C$ in either Equation 1 or Equation 2 with $\log \beta + \log (1/t_f)$. Then at a given temperature S (or S/T) should be linear with $\log (1/t_f)$.

$$S = \frac{(2kT)}{\beta} \ln \beta + \frac{(2kT)}{\beta} \ln \frac{1}{t_f} + \frac{2kT}{\beta} \ln \frac{h_1}{\rho \beta kT} + (2RG\beta)^{1/2} + \frac{2\beta_0}{\beta} \quad (5)$$

or

$$\frac{S}{T} = \frac{(2k)}{\beta} \ln \beta + \frac{(2k)}{\beta} \ln \frac{1}{t_f} + \frac{2k}{\beta} \ln \frac{h_1}{\rho \beta kT} + \frac{(2RG)}{T}^{1/2} + \frac{2\beta_0}{\beta T} \quad (6)$$

Figures 7-10 show that the lines required by Equations 5 and 6 are reasonably linear.

Equations 1, 2, 5, and 6 clearly indicate that the slopes of the lines in Figures 1-4, and 7-10 permit evaluation of β . Table 5 gives values of β determined from each of the four plots at each thickness of aluminum adherend. Average values are summarized in Table 6. Although numerical values of β for the crosslinked modified epoxy are considerably lower than those found by Cherry and Holmes (Ref 3) for polyethylene, β increases with temperature as observed by those investigators.

Some constant stress data for AF126 adhesive used with 1/16 inch aluminum panels is available (Ref 2). In this case, Cherry and Holmes (Ref 3) obtained the relation

$$S = \frac{(-2kT)}{8} \ln t_f + \frac{(2kT)}{8} \ln \frac{h \gamma_f}{\rho \beta kT} + (2RG_e)^{1/2} + 2\sigma_0/8 \quad (7)$$

Equation 7 requires that S be linear with $\log t_f$ with σ readily accessible from the slope as in the case of constant rate of strain experiments. Such a comparison should be useful in giving an indication that the same parameters describe the behavior under differing types of loading. Unfortunately, a direct comparison is not possible since at the long times of the constant stress experiments, the failure time was rather markedly dependent on humidity (Ref 2). Also, at the much lower loads of the constant stress experiments, there was no noticeable deformation of the 1/16 inch aluminum. Hence, a quantitative comparison of σ values for the two cases does not seem to be in order. However, Figures 11-13 show that the constant stress data, allowing for the expected adhesive scatter, does obey Equation 7. This gives some confidence that these relations can describe data obtained by different loading methods. Table 7 gives apparent σ values calculated from the slopes of the lines in Figures 11-13. Qualitatively, the values appear to be in the general range that would be expected from the results described above. However, in each case, there seems to be a rather sharp and unexpected downturn in the σ (increase in slope) curve at the highest temperature (344°K).

EXPERIMENTAL PROCEDURE

Materials

2024-T3 aluminum panels, 4" x 13" x 1/8".

2024-T3 aluminum panels, 4" x 12" x 1/16".

AF126-3, a thermosetting, nonvolatile, modified epoxy film adhesive designed for structural bonding of metals.

Preparation of Adherends

Scribe marks were placed 1/2 inch from the long edge of each panel to assure an accurate overlap of the joint. Two panels were then clamped together in the position for bonding using the scribe marks as a guide. Alignment holes were drilled through the area to be bonded at both ends of the panel. The clamps were then removed and the panels were washed with acetone followed by degreasing in hot vapors of stabilized perchloroethylene. The area to be bonded was then etched for 5 minutes at 150° F in FPL etch solution in accordance with MIL-A-9067C, washed with tap water at 140° F, and rinsed in deionized water. The panels were dried in a forced-air circulating oven at 140° F for one hour.

Preparation of Lap Shear Specimens

One group of panels was prepared using the 1/16 inch thick aluminum adherends and a second group was prepared using the 1/8 inch thick adherends.

A single layer of the film adhesive was placed in the joint and the two adherend panels were pinned in place by putting aluminum rods through the previously drilled holes and hammering the protruding ends flat. Three bonded panels were prepared at one time, overlapping the ends to give them proper support. An extra panel was used for the same purpose under the end of the third bonded panel. The assembly was placed in a hydraulic press at room temperature and subjected to 50 psi pressure. The temperature was raised to 250° F at a rate of approximately 8° F per minute. The pressure and temperature were maintained for one hour. The assembly was then cooled under pressure. These conditions produced a glue line thickness of 2-3 mils. One-inch-wide specimens were cut from the panels with a bandsaw. The pieces from the ends of each panel were discarded.

Specimen Testing

The testing temperatures were maintained by using liquid carbon dioxide and electric heaters as required with a Standard test cabinet. The load was applied with a 60,000-pound Baldwin testing machine operating at a constant rate of crosshead separation. Failure times were measured with a stop watch.

REFERENCES

1. E. McAbee, W. C. Tanner and D. W. Levi, J. Adhesion 2, 106(1970)
2. E. McAbee and D. W. Levi, Prediction of Failure Times of Adhesive Bonds at Constant Stress, PATR 4105, in press.
3. B. W. Cherry and C. M. Holmes, Brit. J. Appl. Phys. (J. Phys. D) 2(2), 821 (1969)

TABLE 1

Failure data for AF126 adhesive with 1/8 inch thick aluminum adherends at constant strain rate

Temperature, °K	Crosshead Separation Rate (C), in./min	S, psi	S/T	t _f , min
193	0.105	6100	31.6	1.608
193	0.8	5330	27.6	0.203
193	2	4540	23.5	0.0805
233	0.105	6310	27.1	1.423
233	0.8	5920	25.4	0.198
233	2	5020	21.5	0.065
273	0.105	6300	23.1	1.508
273	0.8	6060	22.2	0.195
273	2	5050	18.5	0.065
296	0.105	5740	19.4	1.332
296	0.8	5490	18.5	0.190
296	2	4870	16.4	0.060
323	0.105	4860	15.1	1.200
323	0.8	4610	14.3	0.160
323	2	4120	12.8	0.053
343	0.105	3790	11.0	1.140
343	0.8	3920	11.4	0.152
343	2	3540	10.3	0.053

TABLE 2

Failure data for AF126 adhesive with 1/16 inch aluminum adherends at constant strain rate

Temperature, °K	Crosshead Separation Rate (C), in. /min	S, psi	S/T	t _f , min
∞	193	0.105	4760	24.7
	193	0.8	4510	23.4
	193	2	4300	22.3
	233	0.105	5410	23.2
	233	0.8	5280	22.7
	233	2	4800	20.6
	273	0.105	5300	19.4
	273	0.8	5160	18.9
	273	2	4660	17.1
	296	0.105	4880	16.5
	296	0.8	4870	16.5
	296	2	4430	14.9
	323	0.105	4320	13.4
	323	0.8	4280	13.3
	323	2	3810	11.8
	343	0.105	2790	8.1
	343	0.8	2520	7.3
	343	2	2750	8.0
				0.085

TABLE 3

Deformation from C and t_f values

Temperature, °K	C	$\frac{1}{8}$ inch Al	$\frac{\epsilon}{C} = C t_f$ $\frac{1}{16}$ inch Al
193	0.105	0.17	0.15
193	0.8	0.16	----
193	2	0.17	0.22
233	0.105	0.15	0.18
233	0.8	0.16	0.21
233	2	0.13	0.19
273	0.105	0.16	0.17
273	0.8	0.20	0.20
273	2	0.13	0.19
296	0.105	0.14	0.23
296	0.8	0.15	----
296	2	0.12	0.22
323	0.105	0.13	0.16
323	0.8	0.13	0.18
323	2	0.11	0.18
343	0.105	0.12	0.20
343	0.8	0.12	----
343	2	0.11	0.17

TABLE 4

Deformation from $\log C$ versus $\log (1/t_f)$ plots

<u>Temperature, °K</u>	<u>$\log \epsilon$</u>	
	<u>1/8 inch Aluminum</u>	<u>1/16 inch Aluminum</u>
193	-0.77	-0.74
233	-0.86	-0.71
273	-0.86	-0.70
296	-0.88	-0.65
323	-0.95	-0.73
343	-0.96	-0.70

TABLE 5

8 Values from slopes of the various plots

 A^{-3}

<u>Temperature, °K</u>	<u>1/8 inch Aluminum</u>	<u>1/16 inch Aluminum</u>
From S Versus Log C Plots		
193	1470	5150
233	2350	4920
273	2880	5610
296	4350	9250
323	5520	8600
343	7790	10400
From S/T Versus Log C Plots		
193	1480	5150
233	2350	5150
273	3020	5660
296	4230	8650
323	5770	8650
343	9070	11300
From S Versus Log $(1/t_f)$ Plots		
193	1510	4370
233	2350	4690
273	3010	5270
296	4260	7660
323	5860	7910
343	8900	10400
From S/T Versus Log $(1/t_f)$ Plots		
193	1480	4120
233	2350	4780
273	2890	5040
296	4230	7570
323	5290	6760
343	9070	11300

TABLE 6
Variation of average β values with temperature

Temperature, °K	β, A^3	
	1/8 inch Aluminum	1/16 inch Aluminum
193	1500	4700
233	2350	4900
273	2950	5400
296	4300	8300
323	5600	8000
343	8700	11000

TABLE 7

g Values derived from constant stress data

Temperature, °K	g, A ³		
	20% RH	50% RH	95% RH
296	----	----	3800
322	8100	9700	5500
333	9100	10000	7000
344	5200	7800	5900

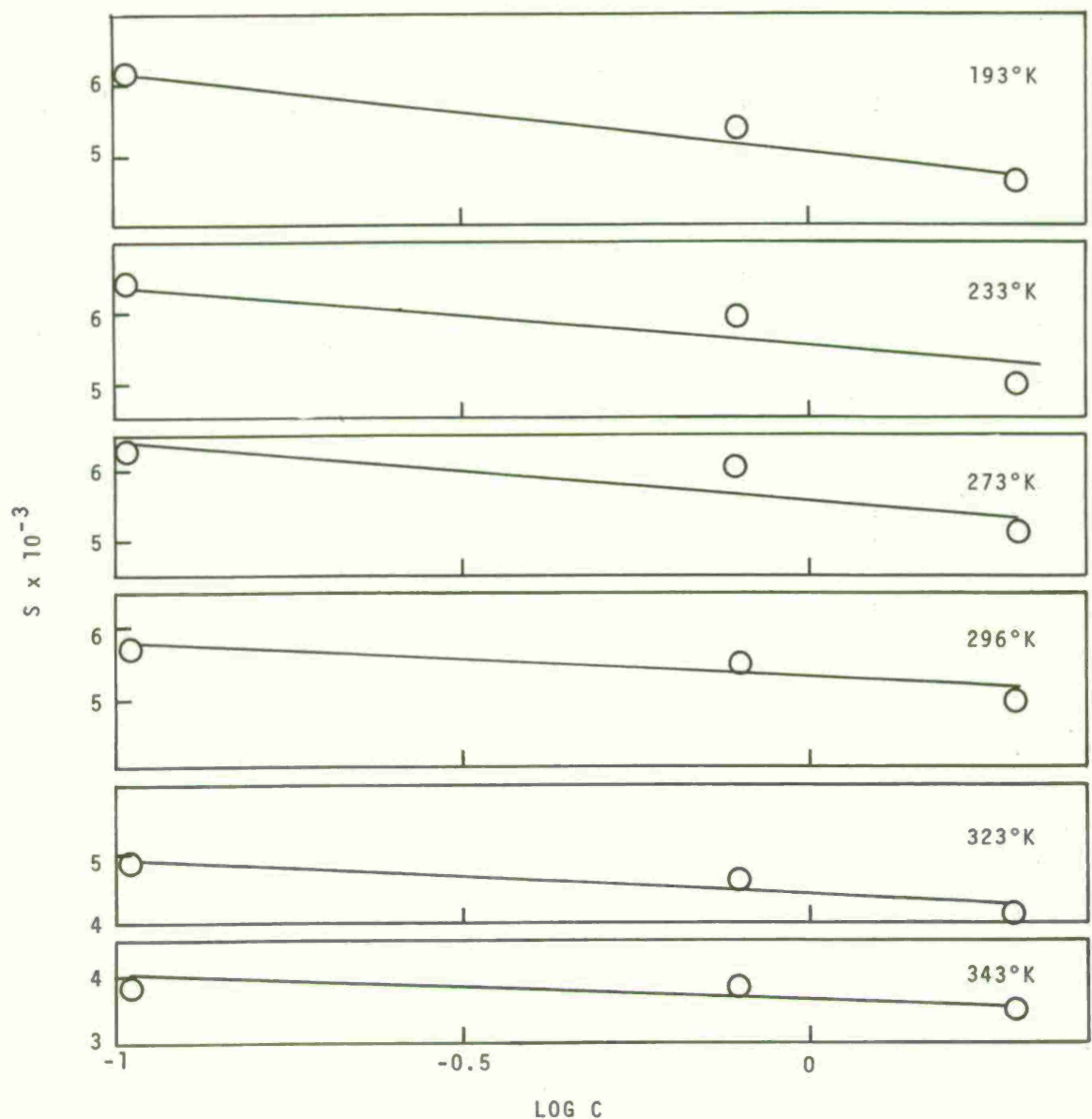


Fig 1 S versus log C for AF126 adhesive with 1/8" aluminum adherends

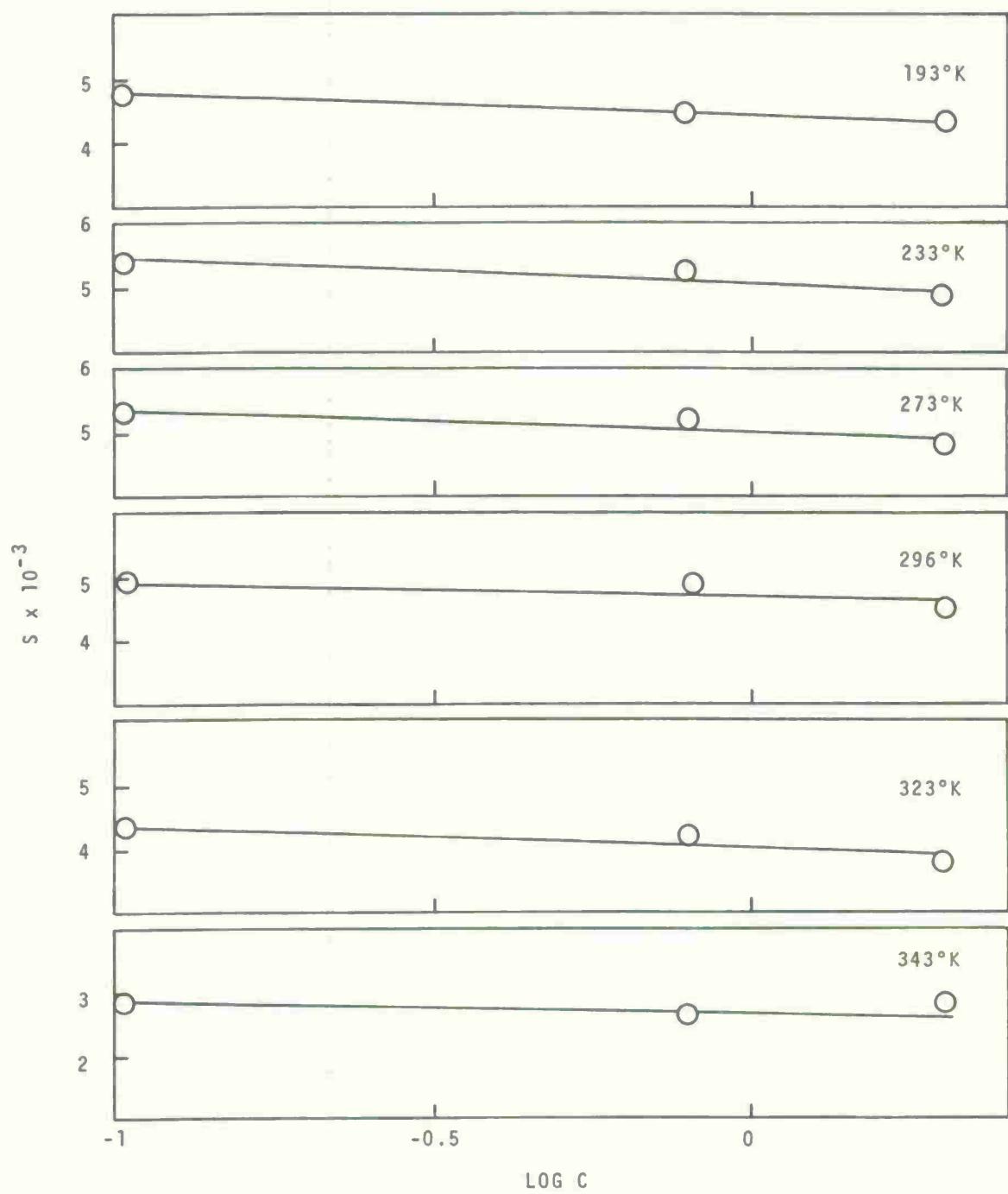


Fig 2 S versus $\log C$ for AF126 adhesive
with 1/16" aluminum adherends

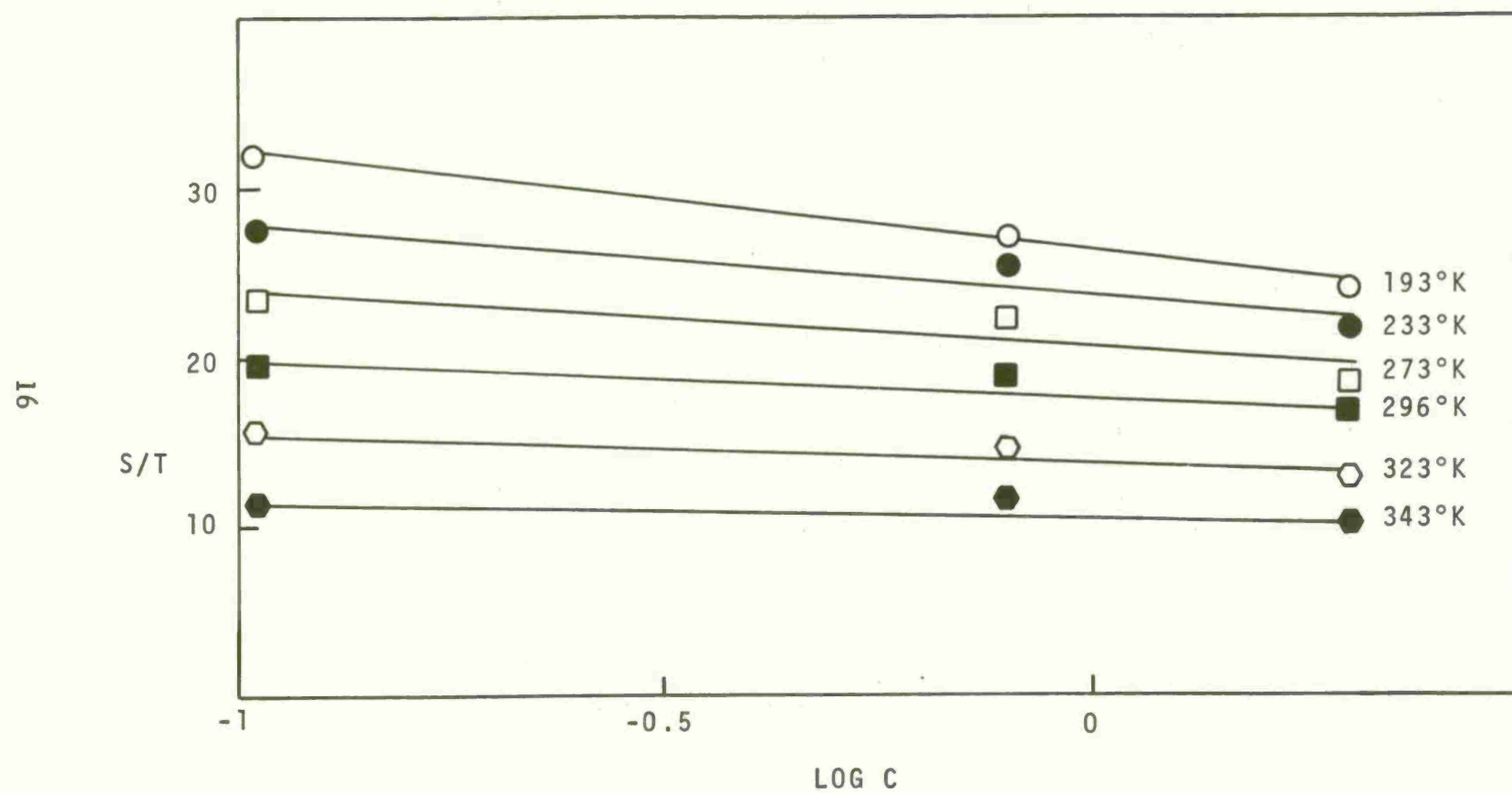


Fig 3 S/T versus log C for AF126 adhesive with $1/8"$ aluminum adherends

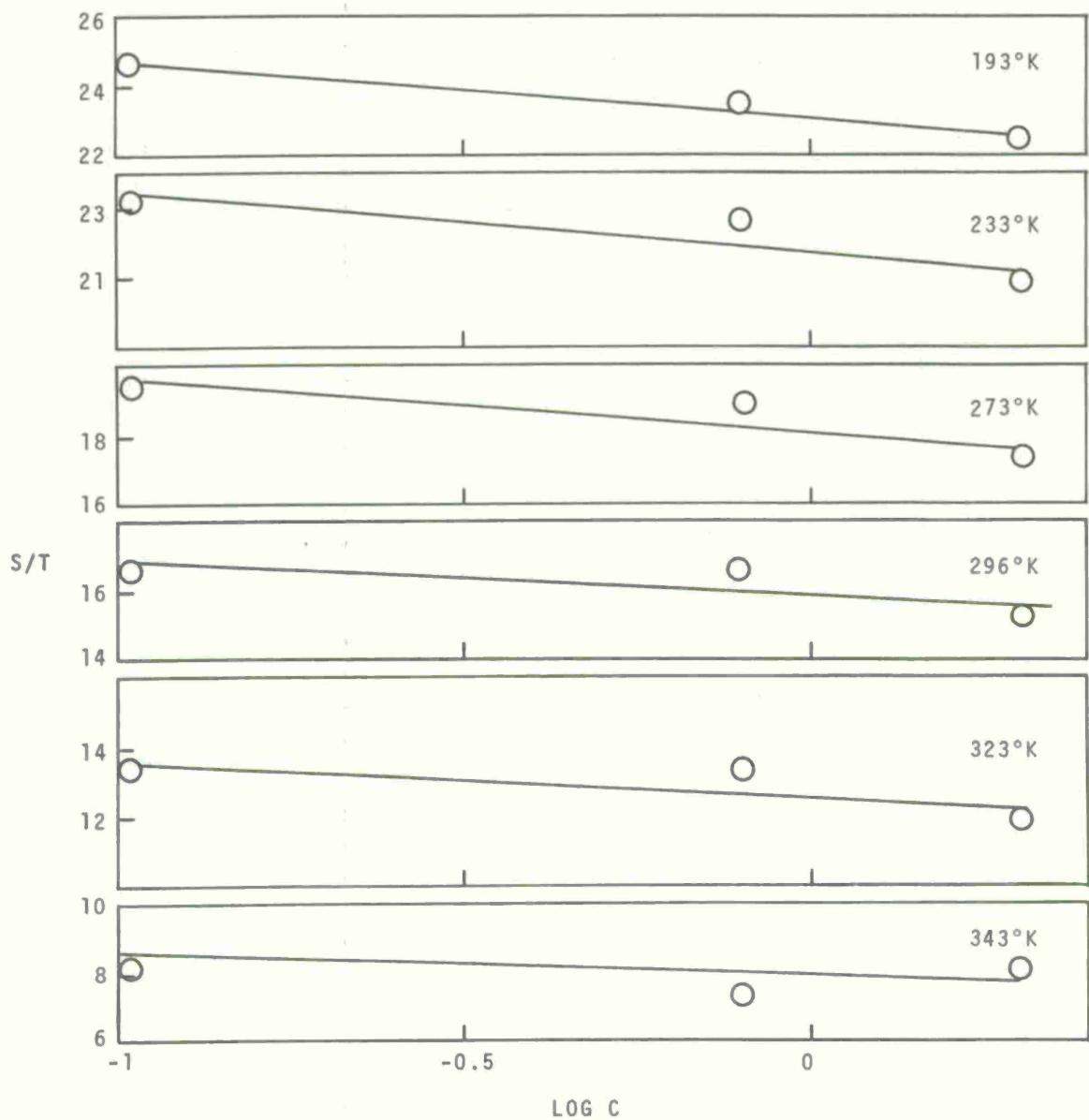


Fig 4 S/T versus log C for AF126 adhesive with 1/16" aluminum adherends

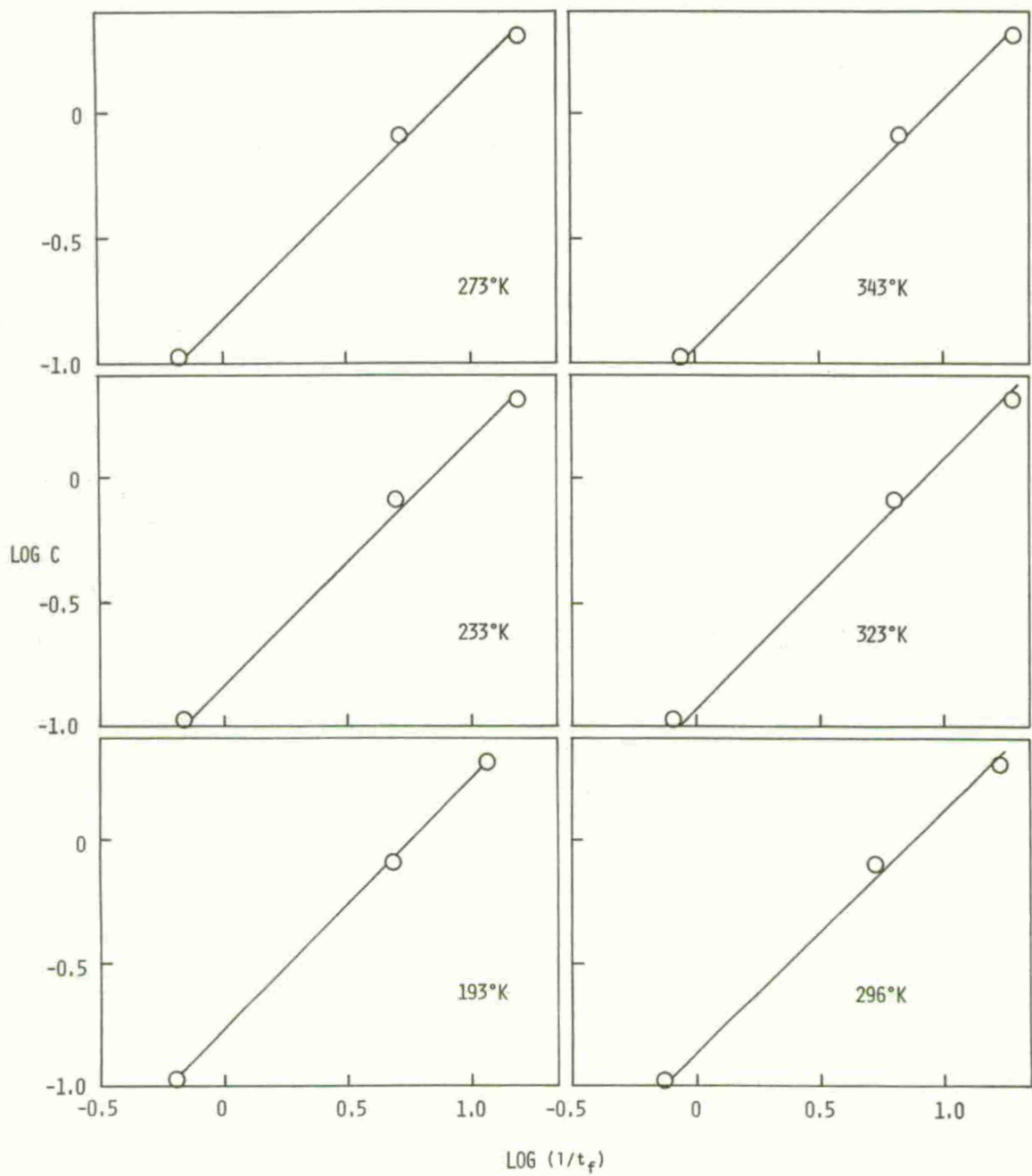


Fig 5 Log C versus $\log (1/t_f)$ for AF126 adhesives with $1/8''$ aluminum adherends

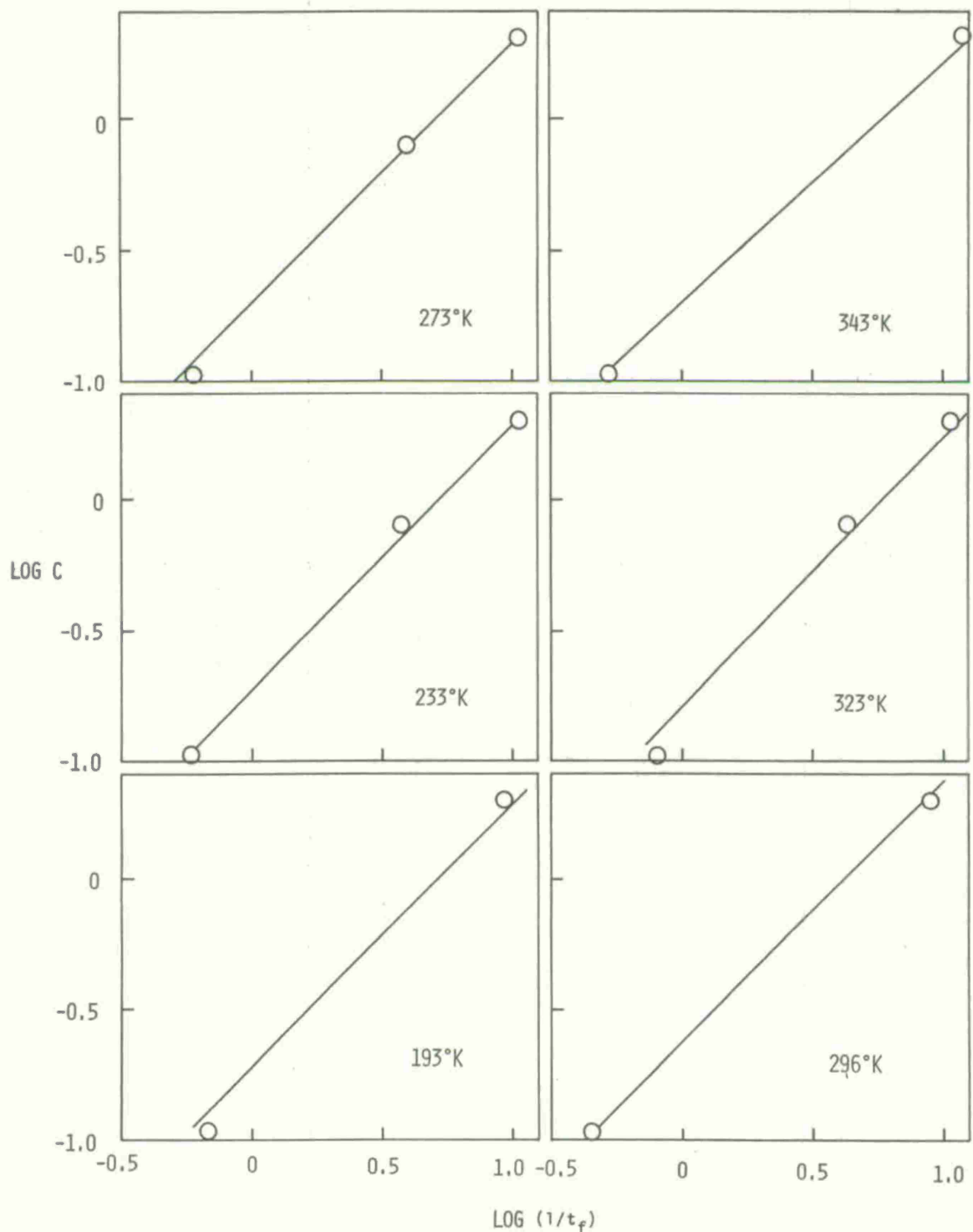


Fig 6 Log C versus $\log (1/t_f)$ for AF126 adhesive with $1/16"$ aluminum adherends

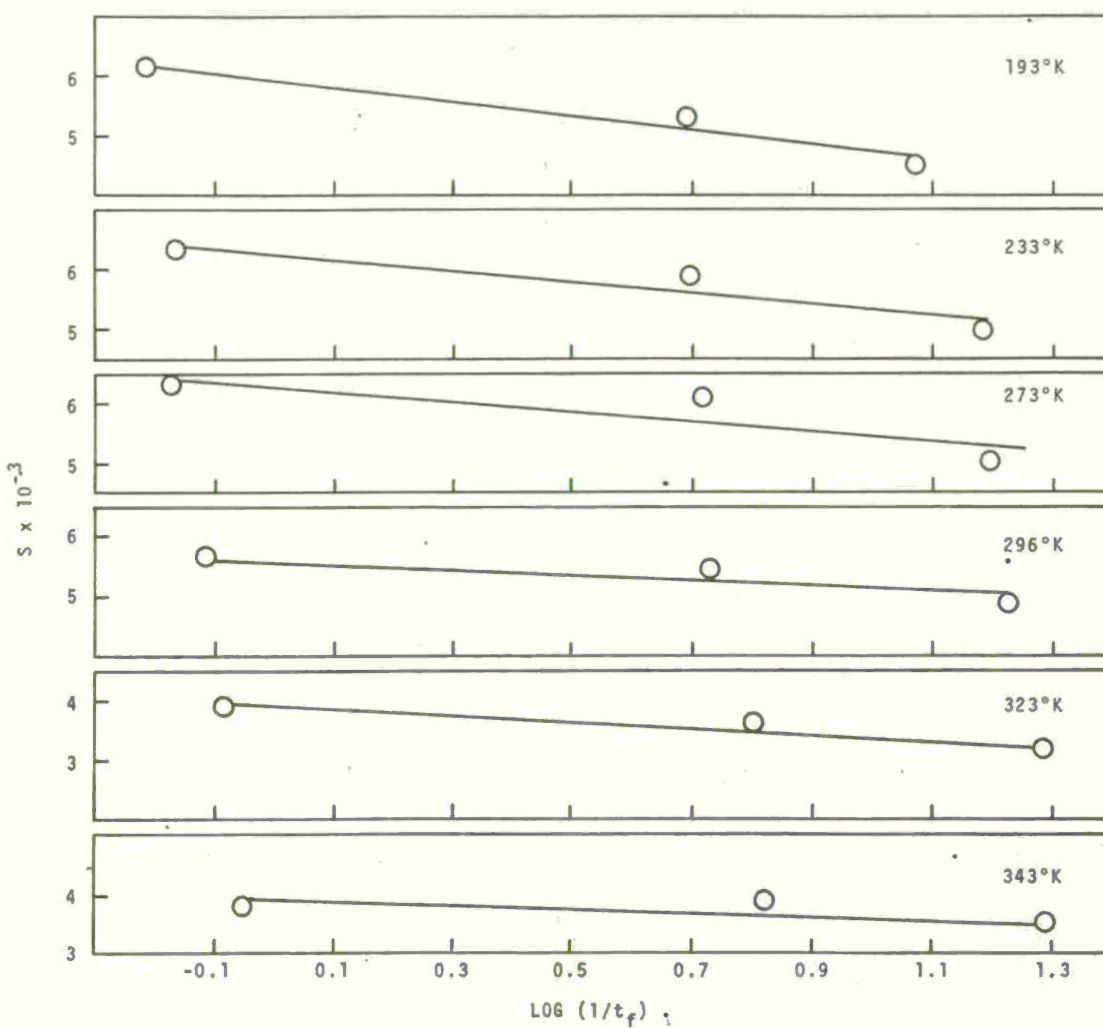


Fig 7 S versus $\log(1/t_f)$ for AF126 adhesive with 1/8" aluminum adherends

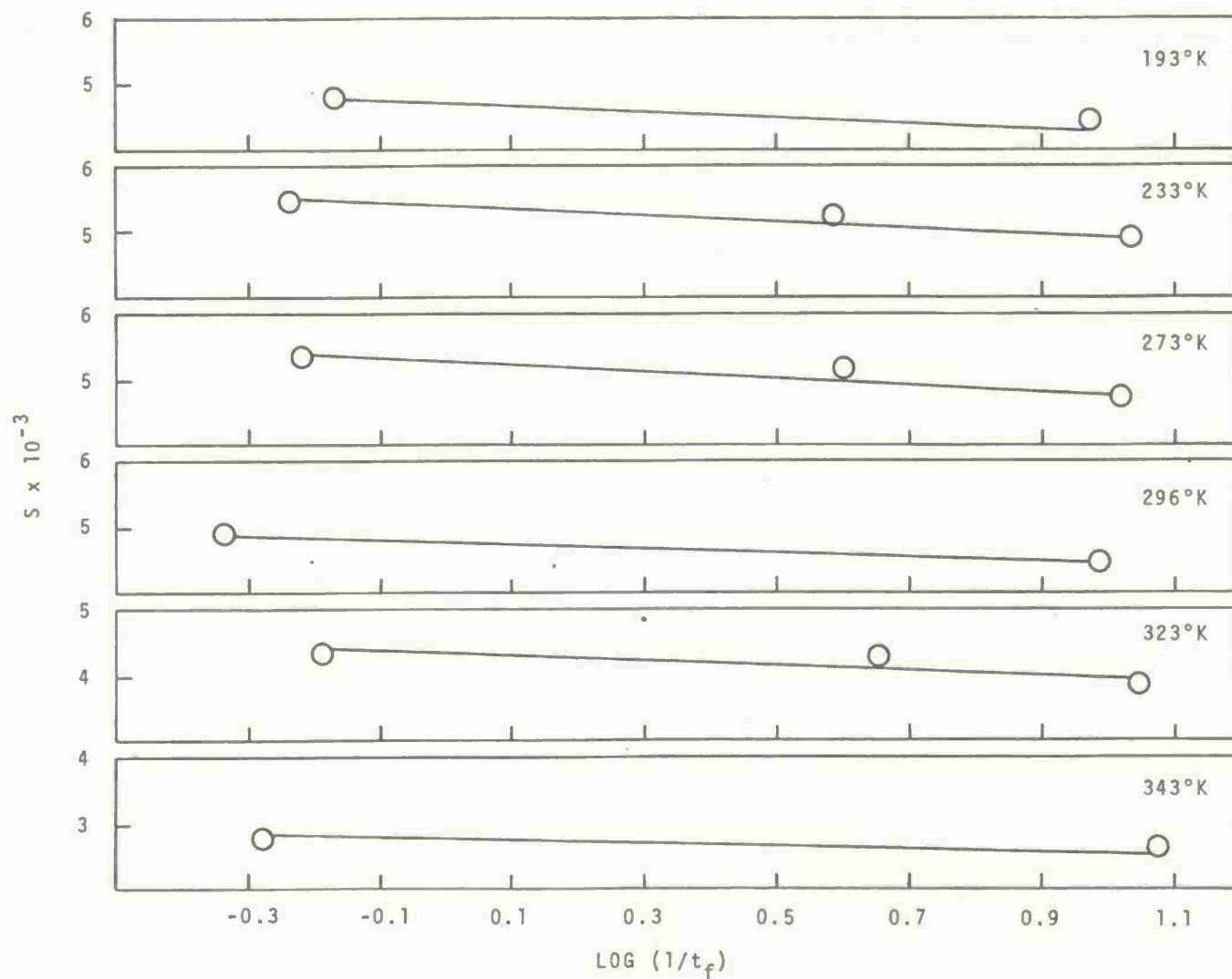


Fig 8 S versus $\text{log } (1/t_f)$ for AF126 adhesive with 1/16" aluminum adherends

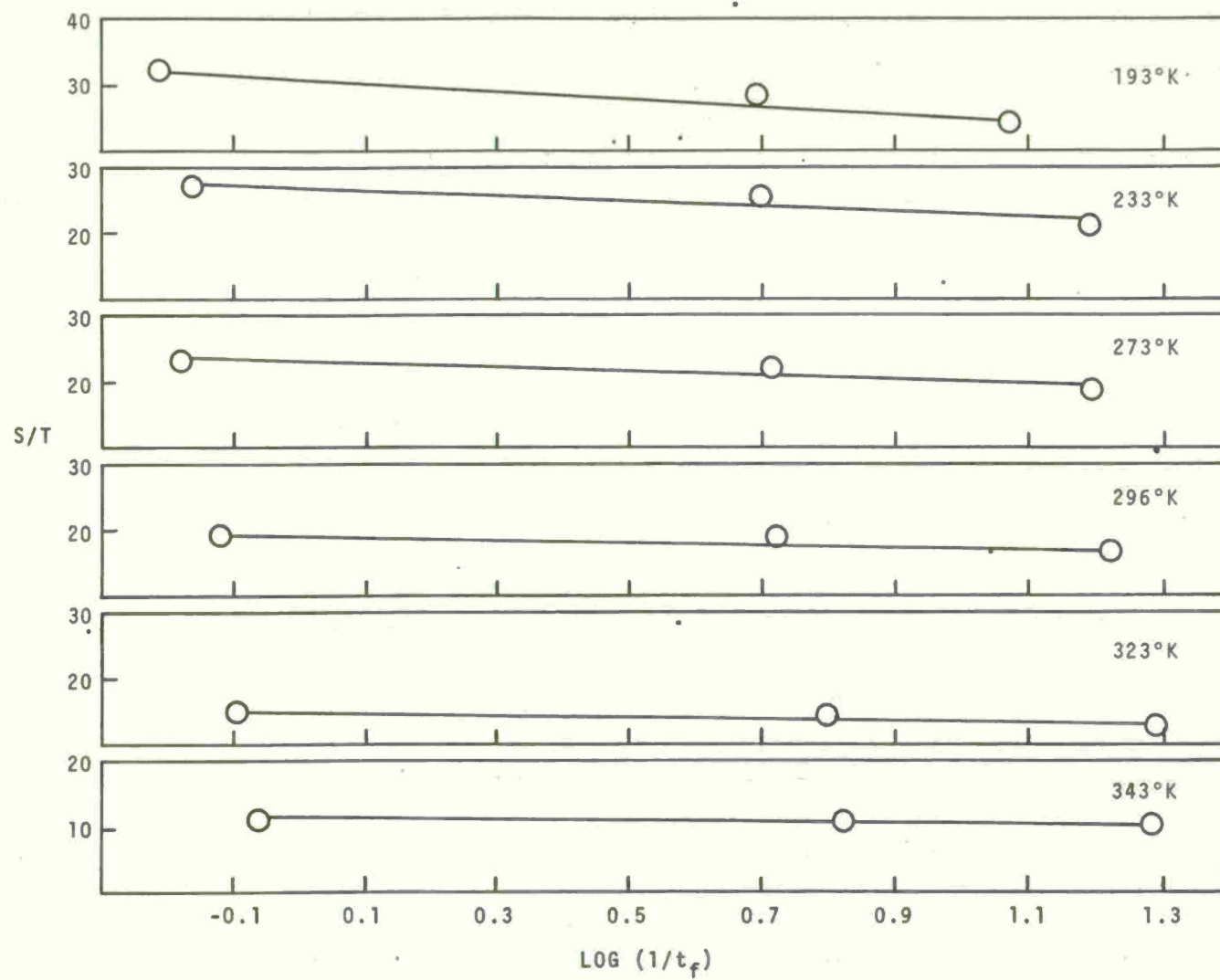


Fig 9 S/T versus $\log (1/t_f)$ for AF126 adhesive with 1/8" aluminum adherends

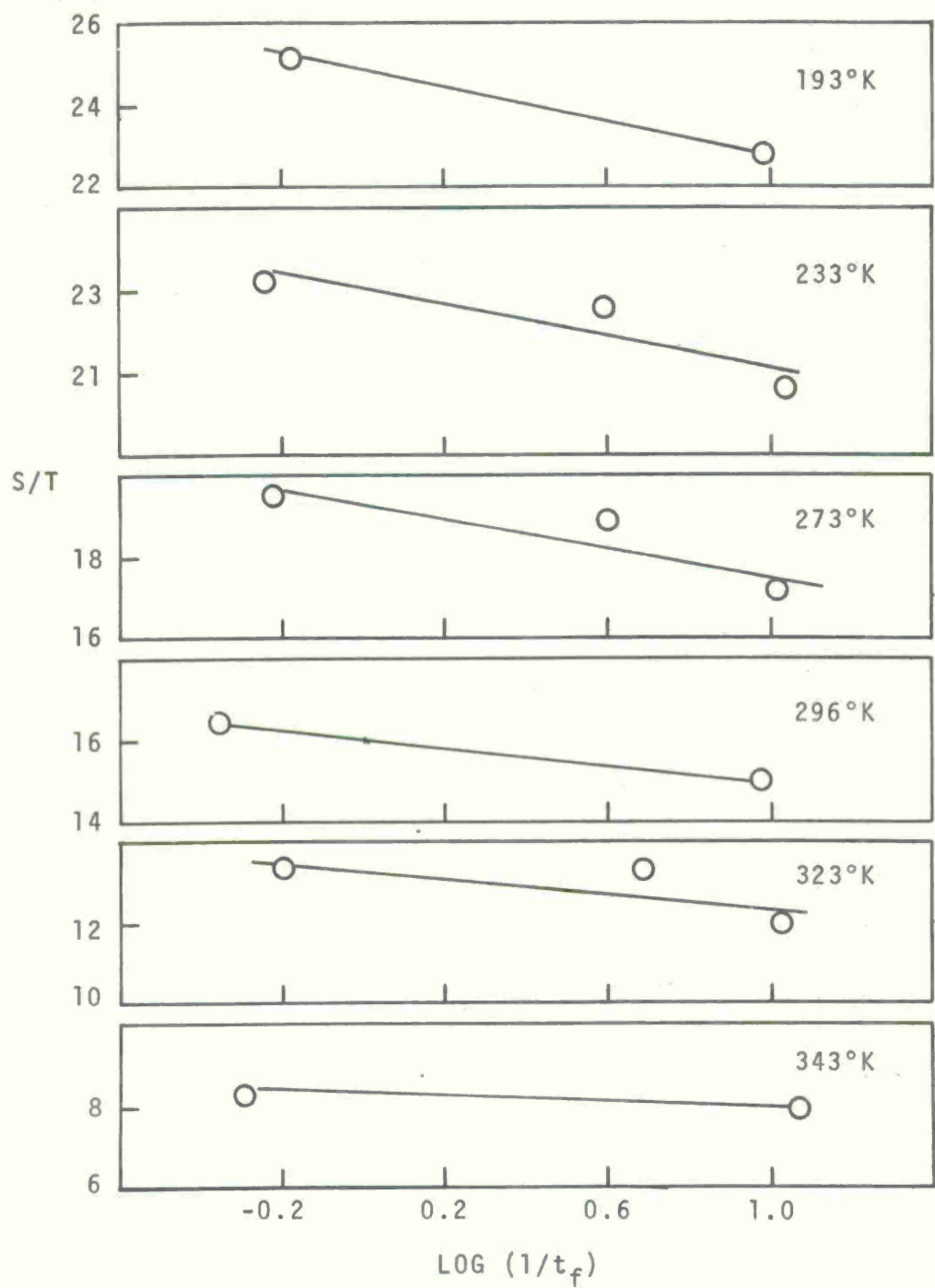


Fig 10 S/T versus $\log (1/t_f)$ for AF126 adhesive
with 1/16" aluminum adherends

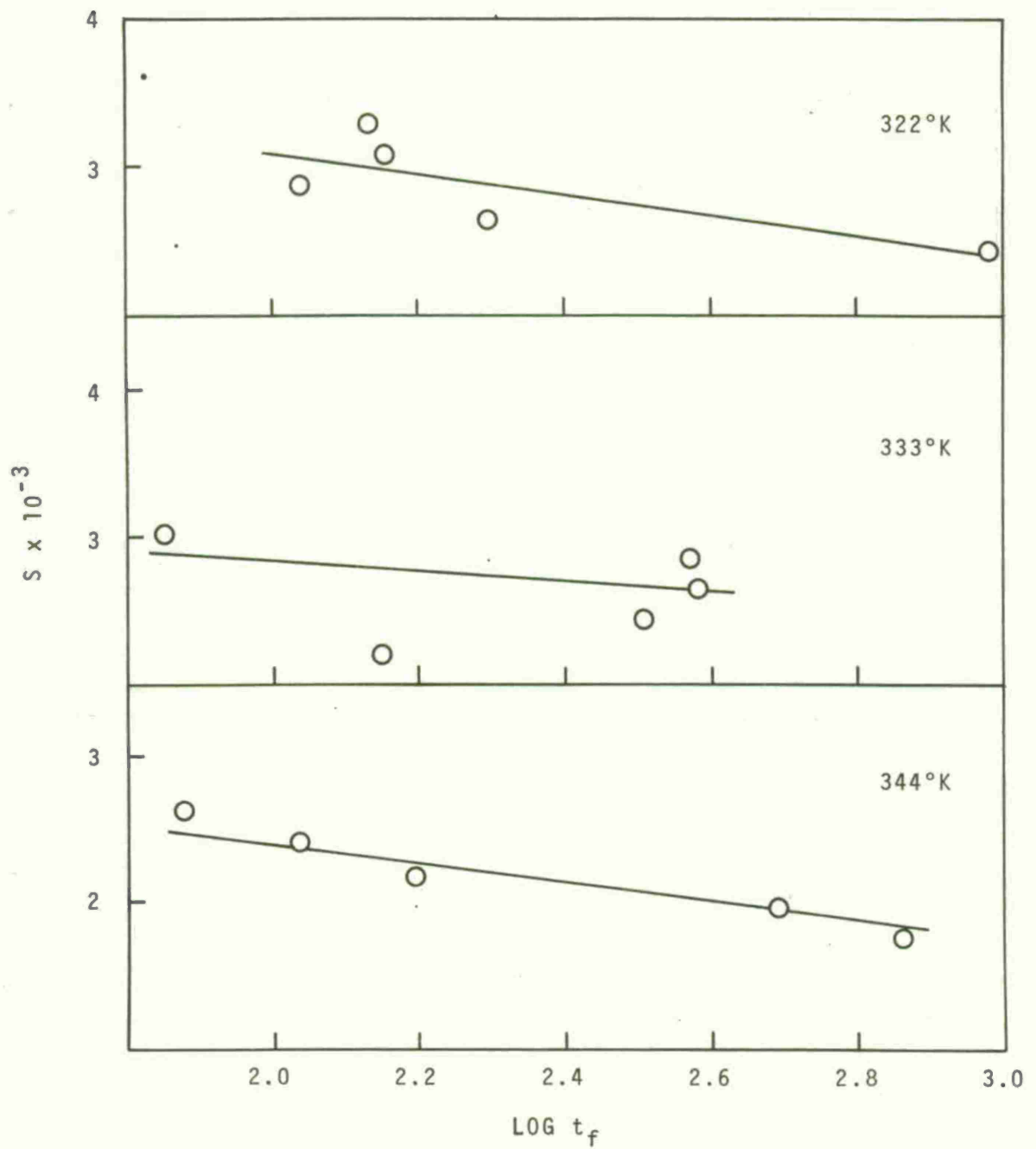


Fig 11 S versus $\log t_f$ for AF126 adhesive
with $1/16"$ aluminum adherends
20% Relative humidity

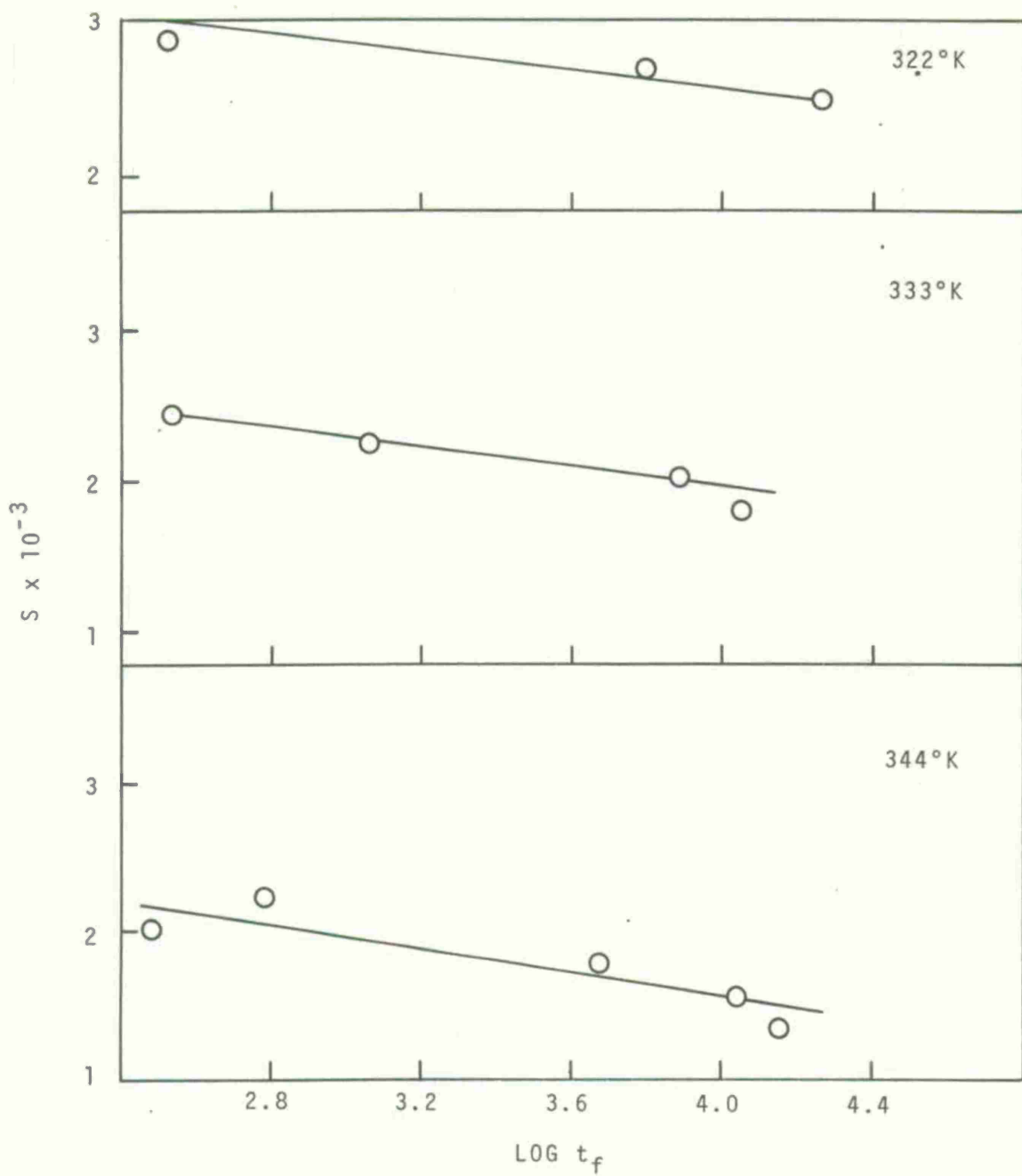


Fig 12 S versus $\log t_f$ for AF126 adhesive
with 1/16" aluminum adherends
50% Relative humidity

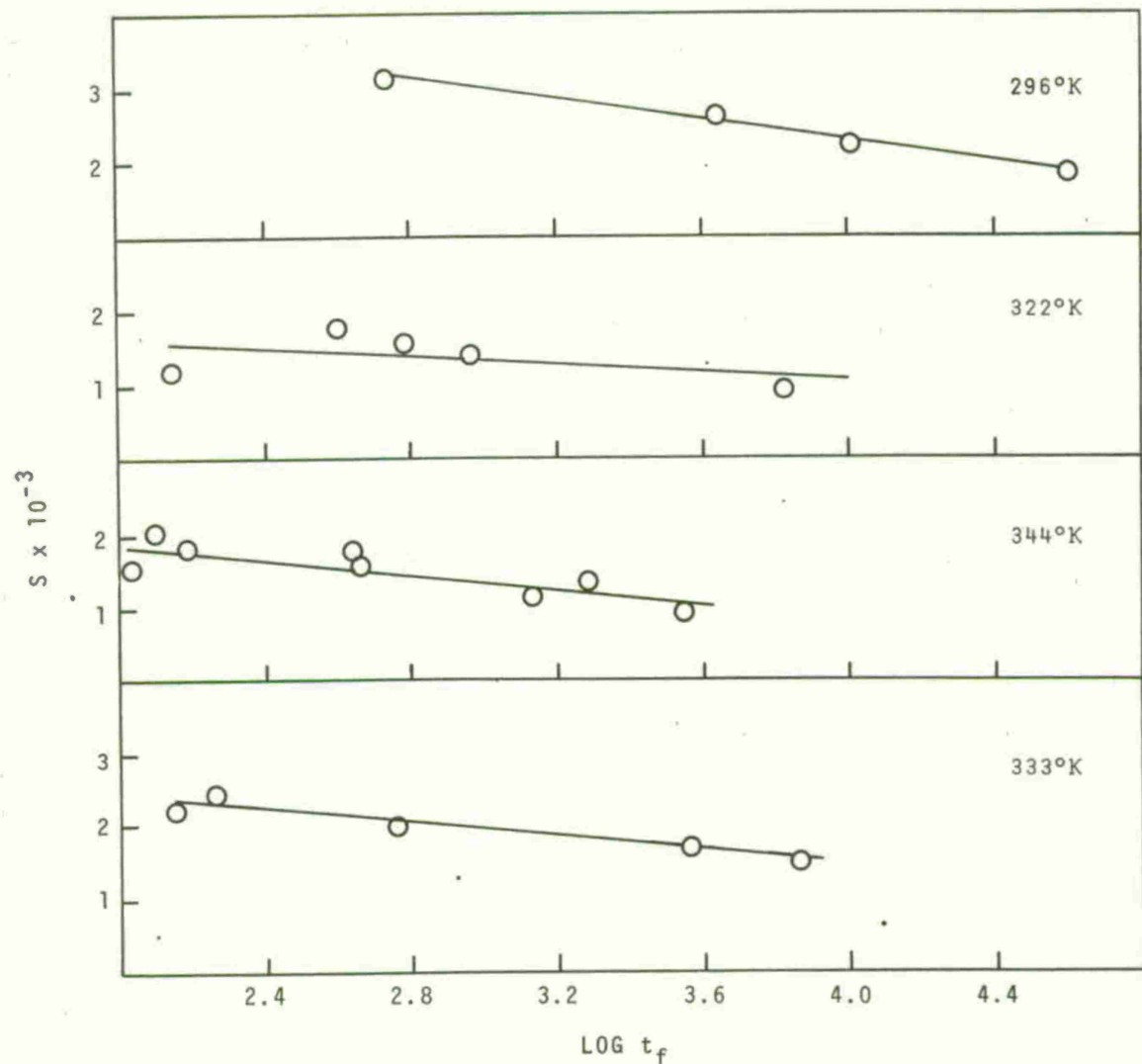


Fig 13 S versus $\log t_f$ for AF126 adhesive
with $1/16"$ aluminum adherends
90-95% Relative humidity

DISTRIBUTION LIST

Copy No.

Commanding Officer

Picatinny Arsenal

ATTN: Scientific and Technical Information Branch	1-6
SMUPA-VP6	7-23
SMUPA-T	24-28
SMUPA-D	29-33
SMUPA-N	34-35
SMUPA-I	36-37
SMUPA-ND	38
SMUPA-NR	39

Dover, New Jersey 07801

Commanding General

U. S. Army Materiel Command

ATTN: AMCRD-T, Dr. H. M. El-Bisi	40
AMCRD-T, Mr. J. Rivkin	41
AMC-PI	42
AMC-QA	43
Physics and Electronics Br., Mr. John Beebe	44

Commanding General

U. S. Army Missile Command

ATTN: AMSMI-IE, Mr. J. E. Kirshstein	45
AMSMI-IEP, Mr. Giles Wetherill	46
AMSMI-RF, Dr. Julian S. Kobler	47
AMSMI-RH, Mr. Gregory S. Moshkoff	48
AMSMI-RL, Mr. William C. Watson	49
AMSMI-RTF, Mr. James M. Taylor	50
AMSMI-RSM, Mr. E. A. Verchot	51
AMSMI-RGP, Mr. Kenneth W. Plunkett	52
AMSMI-IELC, Mr. William B. Greene	53
AMSMI-IELC, Mr. Robert B. Clem	54
AMSMI-IELM-S, Mr. James R. Martin	55
AMSMI-RKK, Mr. C. H. Martin	56
Chief, Document Section	57

Redstone Arsenal, Alabama 35809

Commanding General

U. S. Army Munitions Command

ATTN: AMSMU-RE-E, Mr. E. P. Burke	58
AMSMU-RE-E, Mr. W. G. McDaniel	59
AMSMU-RE-R, Mr. G. Chesnov	60
AMSMU-QA	61
AMSMU-CE, Chief Engineer	62

Dover, New Jersey 07801

Commanding General

U. S. Army Electronics Command

ATTN: AMSEL-PP/P/IED.2, Mr. Wes Karg	63
225 South 18th Street	
Philadelphia, Pennsylvania 19103	

Commanding General

U. S. Army Aviation Systems Command

ATTN: AMSAV-PRL, Mr. John Thorp	64
AMSAV-PPL, Mr. F. Matthews	65
AMSAV-EAA, Mr. R. Rodman	66
AMSAV-R-R(RD), Mr. R. Martin	67
AMSAV-EAC, Mr. J. Bramlet	68
AMSAV-R-R(RD), Mr. W. H. Brabson, Jr.	69
AMSAV-EAS, Mr. R. Reeves	70
AMSAV-EGSM, Mr. A. Taplits	71
AMSAV-R-R(RD), Dr. I. Peterson	72

P.O. Box 209, Main Office

St. Louis, Missouri 63166

Commanding General

U. S. Army Mobility Equipment Command

ATTN: AMSME-PLA, Mr. J. J. Murphy	73
AMSMEM-PLA, Mr. M. W. Schriet	74
4300 Goodfellow Blvd.	
St. Louis, Missouri 63120	

Commanding General	
U. S. Army Tank-Automotive Command	
ATTN: AMSTA-RCM. 1, Mr. Don Phelps	75
AMSTA-RCM. 1, Mr. Edward Moritz	76
Lt. Colonel John W. Wiss	77
Mr. Charles Green	78
Mr. Melvin A. Arvik	79
Warren, Michigan 48090	
Commanding Officer	
U. S. Army Materials and Mechanics Research Center	
ATTN: AMXMR-TX, Mr. Arthur Jones	80
AMXMR-TX, Mr. P. A. Carbonaro	81
AMXMR-RF, Dr. G. Thomas	82
AMXMR-E, Mr. E. Hegge	83
AMXMR-QA	84
Technical Information Section	85
Watertown, Massachusetts 02172	
Commanding Officer	
Savanna Army Depot	
ATTN: AMXSV-EN	86
AMC Ammunition Center	
Savanna, Illinois 61704	
Commanding Officer	
Fort Detrick	
ATTN: SMJFD, Mr. H. H. Meier	87
MD Division, Mr. D. E. Jones	88
MO Branch, Mr. H. Ralph Cunningham	89
Frederick, Maryland 21701	
Commanding Officer	
Rock Island Arsenal	
ATTN: SWERI-PPE-5311, Mr. J. A. Fox	90
AMSWE-PPR, Mr. J. X. Walter	91
AMSWE-PPR, Mr. G. Hall	92
Rock Island Arsenal, Illinois 61201	

Director	
U. S. Army Production Equipment Agency	
Rock Island Arsenal	
ATTN: AMXPE-MT, Mr. H. Holmes	93-94
Rock Island Arsenal, Illinois 61201	
Commanding Officer	
U. S. Army Aeronautical Depot Maintenance Center	
ATTN: SAVAE-EFT, Mr. J. A. Dugan	95
Corpus Christi, Texas 78419	
Project Manager, General Purpose Vehicles	
Michigan Army Missile Plant	
ATTN: AMCPM-GPV-QV, Mr. E. A. Cowgill	96
AMCPM-GPV-T, Mr. L. F. Mortenson	97
Warren, Michigan 48090	
Commanding Officer	
U. S. Army Weapons Command	
Watervliet Arsenal	
ATTN: SMEWV-PPP-WP, Mr. L. Slawsky	98
Dr. Fred Schmiedeshoff	99
Dr. Robert E. Weigle	100
Dr. F. Sautter	101
Mr. W. G. McEwan	102
Mr. P. Rummel	103
Dr. Iqbal Ahmad	104
Watervliet, New York 12189	
Commanding General	
U. S. Army Limited War Laboratory	
ATTN: CRD-AM-6D	105
CRD-AM-7A, Mr. Hugh T. Reilly	106
CRD-AM-6C, Mr. Benjamin F. Wood, Jr.	107
CRD-AM-6C, Mr. R. P. McGowan	108
Aberdeen Proving Ground, Maryland 21005	
Commanding Officer	
Aberdeen Proving Ground	
ATTN: Technical Library, Bldg 313	109
Aberdeen Proving Ground, Maryland 21005	

Commanding Officer	
Harry Diamond Laboratories	
ATTN: Mr. A. A. Benderly	110
Library	111
Washington, D. C. 20438	
Commanding General	
U. S. Army Natick Laboratories	
ATTN: Mr. Theodore L. Bailey	112
Dr. George E. Murray	113
Mr. Jack Furrer	114
Dr. J. Alden Murray	115
Natick, Massachusetts 01760	
Commanding General	
U. S. Army Electronics Command	
ATTN: Mr. J. Spergel	116
Mr. D. A. Diebold	117
Mr. G. Plateau	118
Fort Monmouth, New Jersey 07703	
Commanding Officer	
U. S. Army Engineer Research and Development Labs	
ATTN: Dr. George W. Howard	119
Mr. C. B. Griffis	120
Mr. H. Johnston	121
Mr. E. York	122
Mr. E. B. Holley	123
Fort Belvoir, Virginia 22060	
Commanding Officer	
U. S. Army Edgewood Arsenal	
ATTN: Technical Information Branch	124
Mr. M. A. Raun, SMUEA-DME	125
Mr. N. Potash, SMUEA-DME-4	126
Mr. M. N. Timbs, SMUEA-QAEQ	127
Mr. B. Rogge, SMUEA-WCP	128
Edgewood Arsenal, Maryland 21010	

Commanding Officer	
Frankford Arsenal	
ATTN: Dr. H. Gisser	129
Mr. M. Petronio	130
SMUPA-Q1000	131
Mr. H. Marcus	132
Mr. E. Kelly	133
Philadelphia, Pennsylvania 19137	
Commanding Officer	
Tobyhanna Army Depot	
ATTN: Mr. N. J. DeMars	134
Mr. J. W. Tarrent	135
Tobyhanna, Pennsylvania 18466	
Commanding Officer	
U. S. Army Engineer Waterways Experiment Station	
Corps of Engineers	
ATTN: Mr. Robert Turner	136
Vicksburg, Mississippi 39180	
Commanding General	
U. S. Army Medical Biomechanical Research Laboratory	
Water Reed Army Medical Center	
ATTN: Dr. Fred Leonard	137
Forest Glen Section	
Washington, D. C. 20012	
Commanding General	
U. S. Army Medical Equipment Research and	
Development Laboratory	
Fort Totten	
ATTN: Mr. Donald O. Jones	138
Mr. Aaron Ismach	139
Flushing, Long Island, New York 11359	
Plastics Technical Evaluation Center	
ATTN: Mr. H. Pebly	140
Picatinny Arsenal	
Dover, New Jersey 07801	

Commanding General
White Sands Missile Range
ATTN: Technical Library
New Mexico 88002 141

Commanding Officer
Ammunition Procurement and Supply Agency
ATTN: AMUAP-QFO 142
Joliet, Illinois 60436

U. S. Naval Ordnance Laboratory
ATTN: Mr. F. R. Barnet 143
Silver Spring, Maryland 20910

Department of the Navy
Bureau of Naval Weapons
ATTN: RRMA, Airborne Equipment Division 144
Washington, D. C. 20360

Mr. D. M. McLeod, Supt. Materials Division
Naval Air Engineering Center
Building 76-5
Philadelphia, Pennsylvania 19112 145

Department of the Navy
Bureau of Naval Weapons
ATTN: RRMA-10 146
Washington, D. C. 20360

Naval Air Development Center
Aeronautical, Electronic and Electrical Laboratory
ATTN: Materials and Process Branch 147
Johnsville, Pennsylvania 18974

Naval Ship Research and Development Center
ATTN: Materials Research Branch 148
Washington, D. C. 20007

Defense Documentation Center Cameron Station Alexandria, Virginia 22314	149-159
U. S. Army Aviation Material Laboratory ATTN: Mr. Roach Fort Eustis, Virginia 23604	160
Commander Aeronautical Systems Division ATTN: Mr. R. T. Schwartz Mr. R. C. Tomashot Mr. T. Reinhart	161 162 163
Wright-Patterson Air Force Base, Ohio 45433	
Commanding General Headquarters, U. S. Air Force Pentagon Building Washington, D. C. 20330	164
National Aeronautics and Space Administration Lewis Research Center ATTN: Ch, Library 21000 Brookpark Road Cleveland, Ohio 44135	165
NASA Scientific and Technical Information Facility Information Retrieval Branch ATTN: Mr. William Neely P. O. Box 33 College Park, Maryland 20740	166
U. S. Army Research Office ATTN: Dr. J. M. Majorwicz 3045 Columbia Pike Arlington, Virginia 22204	167
Director U. S. Army Ballistics Research Laboratory ATTN: Mr. Emerson V. Clarke, Jr. Dr. Eichelberger Mr. Herman P. Gay	168 169 170
Aberdeen Proving Ground, Maryland 21005	

Naval Underwater Weapons Station Research Department ATTN: Mr. F. Spicola Newport, Rhode Island 02840	171
Naval Air Systems Command Industrial Resources Branch ATTN: Mr. P. Robinson Washington, D. C. 20360	172
Naval Electronic Laboratory Center ATTN: Mr. Harvey F. Dean, Code S-340 San Diego, California 92152	173
Naval Ordnance Systems Command Industrial Resources Division ATTN: Mr. T. E. Draschil, Code 0471E Washington, D. C. 20360	174
U. S. Navy Ships Systems Command Hdqtrs. ATTN: Mr. T. Kelley, Code 703A Annapolis Academy Annapolis, Md. 21402	175
Naval Research Laboratory ATTN: Mr. W. Oaks, Code 2343 Washington, D. C. 20390	176
Naval Ordnance Station ATTN: Mr. T. Peake Southside Drive Louisville, Ky. 40214	177
Naval Avionics Facility ATTN: Mr. B. D. Togue, Code D/803 21st and Arlington Indianapolis, Ind. 46218	178
Naval Material Industrial Resources Office ATTN: Mr. L. F. Walton Mr. H. Shapiro Philadelphia, Pa. 19112	179 180

Commanding General	
U. S. Army Materiel Command	
ATTN: Mr. J. Dockins, AMCPM-UA-T	181
Mr. C. Cioffi, AMCPM-LH-T	182
P. O. Box 209	
St. Louis, Mo. 63166	
Headquarters	
U. S. Air Force (AFRDDA)	
Washington, D. C. 20330	183
Headquarters	
Air Force Armament Laboratory (ATX)	
Eglin Air Force Base, Florida 32542	184
Headquarters	
Air Force Systems Command (SCTS)	
Andrews Air Force Base, Md. 20331	185
Headquarters	
Air Force Weapons Laboratory (WLX)	
Kirtland Air Force Base, N. M. 87117	186
Deputy Commanding General	
U. S. Army Munitions Command	
ATTN: AMSMU-MM-B	
Joliet, Illinois 60436	187

UNCLASSIFIED

Security Classification

DOCUMENT CONTROL DATA - R & D

(Security classification of title, body of abstract and indexing annotation must be entered when the overall report is classified)

1. ORIGINATING ACTIVITY (Corporate author)		2a. REPORT SECURITY CLASSIFICATION UNCLASSIFIED
Picatinny Arsenal, Dover, N. J.		2b. GROUP
3. REPORT TITLE FAILURE OF ADHESIVE BONDS AT CONSTANT STRAIN RATES		
4. DESCRIPTIVE NOTES (Type of report and inclusive dates)		
5. AUTHOR(S) (First name, middle initial, last name) Elise McAbee, Michale J. Bodnar, William C. Tanner and David W. Levi		
6. REPORT DATE MARCH 1971	7a. TOTAL NO. OF PAGES 41	7b. NO. OF REFS 3
8a. CONTRACT OR GRANT NO.	8b. ORIGINATOR'S REPORT NUMBER(S) Technical Report 4152	
b. PROJECT NO. c. AMCMS Code 4010.28.9.02003	9b. OTHER REPORT NO(S) (Any other numbers that may be assigned this report)	
10. DISTRIBUTION STATEMENT Approved for public release; distribution unlimited.		
11. SUPPLEMENTARY NOTES	12. SPONSORING MILITARY ACTIVITY	
13. ABSTRACT Shear strengths of adhesive AF126 bonds to two thicknesses of aluminum were measured at constant rate of crosshead separation. Primarily cohesive failure was observed in all cases. By using relations proposed by Cherry and Holmes, the shear strength could be quantitatively related to temperature and strain rate or failure time. Of specific engineering interest would be the possibility of determining the reliability of a bonded joint for specific periods of time as a function of continuously applied stress at a given temperature.		

DD FORM 1 NOV 68 1473

REPLACES DD FORM 1473, 1 JAN 64, WHICH IS
OBSOLETE FOR ARMY USE.**UNCLASSIFIED**

Security Classification

UNCLASSIFIED

Security Classification

14. KEY WORDS	LINK A		LINK B		LINK C	
	ROLE	WT	ROLE	WT	ROLE	WT
Adhesive bonds, failure of Constant strain rates AF126 adhesive Aluminum (2024-T3) adherends, 1/8 inch Aluminum (2024-T3) adherends, 1/16 inch Lap shear specimens Temperature effects (193°, 233°, 273°, 296°, 323°, 343K) RH effects (20%, 50%, 90-95%) Shear strength of structural adhesives Deformation of adherends Preparation of adherends Preparation of specimens Test procedures						

UNCLASSIFIED

Security Classification

